Biochemical and Biophysical Research Communications 438 (2013) 519–525

Contents lists available at ScienceDirect

Biochemical and Biophysical Research Communications

journal homepage: www.elsevier.com/locate/ybbrc

Shadoo binds lipid membranes and undergoes aggregation and fibrillization

Qiaojing Li [a], Christophe Chevalier [a], Céline Henry [b], Charles-Adrien Richard [a], Mohammed Moudjou [a], Jasmina Vidic [a,*]

[a] Virologie et Immunologie Moléculaires – INRA, Jouy en Josas, France
[b] Protein Structure and Biochemistry – INRA, Jouy en Josas, France

ARTICLE INFO

Article history:
Received 17 July 2013
Available online 1 August 2013

Keywords:
Lipid-membrane
Shadoo
Circular dichroism
Amyloid fibers
Membrane perturbation
Electron microscopy

ABSTRACT

Lipid membrane can enhance prion protein (PrP) pathological fibrillogenesis. A neuronal paralog of PrP, named Shadoo (Sho), is localized to similar membrane environment as PrP and can also convert to amyloid-like fibrilles. To gain insight into the role of Sho in prion diseases, we studied Sho interactions with cellular membrane models. Sho was found to bind anionic lipid vesicles. Spectroscopic and microscopic data showed that membrane-associated Sho slowly converted into amyloid fibers. Furthermore, binding of Sho to anionic liposomes has a disruptive effect on the integrity of the lipid bilayer leading to the formation of supramolecular lipid–protein complexes. In consequence, the role of Sho in prion diseases might depend on the oligomerization state of Sho but also the nature of these lipoprotein assembles.

1. Introduction

Prion diseases are fatal neurodegenerative disorders that include bovine spongiform encephalopathy in cattle, scrapie in sheep, and variant Creutzfeld–Jacob disease in human. They are associated with aggregation of the prion protein (PrP) into oligomers and amyloid fibers. Prior to aggregate, cellular PrP (PrP^{C}), mainly composed of α-helix, undergoes an α-to-β transition into an abnormal scrapie isoform (PrP^{Sc}) [1,2]. A domain of two α-helixes and/or the protein hydrophobic domain (HD) are reported to be involved in the conformational switch, which can act as an aggregation seed for the conversion [3]. In contrast, the non-structured N-terminal domain of PrP is proposed to play a role in early stages of polymerization by increasing local protein concentration on some cell membranes [4,5].

Although PrP seems to be the major agent in prion pathologies, some other biomolecules were proposed to be essential to infectivity. Firstly, conversion from PrP^{C} to PrP^{Sc} is thought to take place at the plasma membrane or on endosomes/lysosomes [6]. This suggests that some membrane lipids may be involved in the conversion. Secondly, prion protein family contains two paralogs of PrP: Doppel and Shadoo (Sho) [7]. Doppel is unable to undergo a characteristic α-to-β conversion and to attain misfolded and aggregated states. In contrast, Sho was showed to form amyloid-structured aggregates under physiological conditions [8]. Sho shows some sequence homology to HD and N-terminal domains of PrP^{C} and is an unstructured protein in aqueous solutions [8].

The structural homologies and similar brain distribution of PrP and Sho suggested that these two proteins may share the same function in neuronal cells. Indeed, both PrP and Sho have some neuroprotective properties. Expression of Sho is down regulated in prion infected mice [9]. However, Sho levels are unchanged in the brains of adult mice lacking PrP^{C} [10]. Finally, Sho overexpression does not influence the kinetics of prion replication in mice [11].

Since lipid–protein interactions can favor PrP fibrilization, we investigated Sho amyloid fiber formation upon binding to model lipid membranes. We found that Sho binds negatively charged but not zwitterionic liposomes. Upon binding, Sho destabilizes vesicle structure, undergoes aggregation and amyloid fiber formation.

2. Materials and methods

2.1. Reagents and antibodies

Phosphatidylserine (PS) and Phosphatidylcholine (PC) were purchased from Avanti Polar Lipids (AL, USA). Other reagents were purchased from Sigma–Aldrich (France). Following buffers were used: 20 mM citrate buffer, pH 3.35; 5 mM sodium-acetate buffer, pH 5;

* Corresponding author. Address: Virologie et Immunologie Moléculaires, INRA, 78350 Jouy en Josas, France. Fax: +33 1 34652621.
E-mail address: jasmina.vidic@jouy.inra.fr (J. Vidic).

0006-291X/$ - see front matter © 2013 Elsevier Inc. All rights reserved.
http://dx.doi.org/10.1016/j.bbrc.2013.07.104

5 mM ammonium-acetate buffer, pH 5; 20 mM MES buffer, pH 6; 20 mM MOPS acid buffer, pH 7 and 20 mM MOPS buffer, pH 8.

2.2. Plasmid constructs and expression of proteins

The gene encoding mouse Sho (Sho^{25-122}) was cloned in pET-28 plasmid (Novagen) and expressed in SolBL21 *Escherichia coli* (Genlantis). Expression was induced overnight by adding IPTG (240 mg/L) to a culture of bacteria in Luria–Bertanimedium supplemented with kanamycin (40 mg/L) in the shaking incubator at 37 °C. Genes of full-length PrP sheep variant ARQ (PrP^{24-234}), and of its N-terminal peptide (Nter-PrP^{24-134}) were cloned in pET 22b+ and expressed by ITPG induction in the BL21 DE3 *E. coli* strain as previously presented [5].

2.3. Protein purification

Recombinant His_6-tagged Sho was accumulated in bacteria inclusion bodies. Bacteria were lysed in 0.1% Triton X-100, 2 μM EDTA, 50 mM Tris–HCl buffer, pH 7.5 for 15 min at 37 °C, and sonicated for 5 min on ice. Inclusion bodies were separated by centrifugation, and solubilized in 6 M Guanidine-HCl, 20 mM Tris–HCl, 0.5 M NaCl, pH 7.4 overnight at 4 °C. Sho was purified by a two-step method using a Nickel sepharose IMAC column and a size exchange chromatography (AKTA, FPLC, GE Healthcare). After HiTrap IMAC column equilibrion with 20 mM Tris–HCl, pH 7.4, 0.5 MNaCl, 8 M Urea, 5 mM Imidazole, the supernatant was loaded on the column with a 50 mL-superloop. A 15 min Imidazole linear gradient (80–800 mM) in the same buffer was applied to elute the column-bound proteins. One-ml fractions were collected, subjected to 12.5% SDS–PAGE electrophoresis and stained by Coomassie Blue. The Sho–Histag containing fractions were pooled and subjected to size exclusion chromatography on Superdex 200 column equilibrated with 20 mM Tris–HCl buffer pH 7.4, 0.5 M NaCl, 8 M Urea. One-ml fractions were collected and checked for Sho by SDS–PAGE. Nter-PrP, and PrP were purified by a one-step method as explained before [5]. All proteins were recovered in 0.5 g/L ammonium-acetate buffer, pH 5, by elution through a G25 desalting column (Hi TrapTM, GE Healthcare), lyophilized and stored at −20 °C. The final protein concentration was determined by measuring absorbance at 280 nm on Nanodrop 2000c (Labtech, France).

2.4. Liposome preparation

Lipids (10 mg) were solubilized in chloroform and their dry films were obtained by chloroform evaporation under a stream of nitrogen. The lipid film was hydrated with 10 ml of 5 mM sodium acetate buffer, pH 5, and gently vortex and sonicated for a few minutes. The liposomes were than freezed/thawedthree times in liquid nitrogen (vortex between every defrosting) and subsequently extruded through a polycarbonate membrane filter (MILLIPORE 0.1 μm) to obtain small size liposomes.

2.5. Giant liposome preparation and fluorescent microscopy

Lipid film obtained from lipids solubilized in chloroform was hydrated with 5 mM sodium acetate buffer, pH 5. The obtained solution was rested for 2 h at 37 °C and then kept at 4 °C before use. For fluorescence microscopy, giant liposomes were stained with ThT (10 μM) for five minutes and visualized with an inverted UV–visible light microscope (Carl Zeiss). Obtained images were analyzed using Axiovision (Zeiss).

2.6. Fluorescence spectroscopy of tryptophan

Fluorescence measurements were performed with a FP-6200 spectrofluorimeter (JASCO, Tokyo, Japon) connected with a thermostatted cell holder at 20 °C, using a 1-cm path length quartz cell. The maximum emission wavelength (λ_{max}) represents the average of three values obtained from emission spectra that were correlated for blank measurements.

2.7. Thioflavin T (ThT) assay

Thioflavin T (ThT) binding assays were recorded in FP-6200 spectrofluorimeter at 20 °C. Protein samples were preincubated with ThT (100 μM) for 5 min at room temperature before measurements. Fluorescence spectra were measured from 470 to 600 nm, using an excitation wavelength of 435 nm, at an 1-cm path length quartz cell.

2.8. Ultracentrifugation

Recombinant proteins (15 μM) were incubated with PC or PS (0.3 mg/mL) liposomes for 2 weeks at 4 °C. The samples were then ultracentrifuged at 40,000×*g* for 40 min (BECKMAN TL-100, USA). A 10-μL aliquot of each sample, containing either soluble or a lipids-bound fraction was resuspended in Laemmli buffer and heated for 5 min at 100 °C. Proteins were analyzedby SDS–PAGE and stained with Coomassie Blue.

2.9. Circular dichroism

Far-UV (180–260 nm) CD spectra were measured on a JASCO J-810 spectropolarimeter using 1 mm path length quartz cell. Spectra were collected at a scanning rate 100 nm/min, a bandwidth1.0 nm and a resolution of 100 mdeg and corrected for the contribution of the buffer. Measurements were done at 20.

2.10. Electronic microscopy

20 μM Sho incubated with1 mg/ml liposomes was collected on formvar-coated copper grids (Agar, Oxford Instruments). After being rinsed twice for 1 min in PBS, samples were negatively stained with 2% uranyl acetate (Ladd Research Industries) for 1 min. The grids were air dried before observation under a Zeiss EM902 TEM operated at 80 kV (Carl Zeiss, France)

2.11. DLS analysis

Sizes of protein and liposome were checked by Zetasizer Nano serie ZEN-1600 (Malvern Instruments, UK) based on dynamic light scattering (DLS). For each measurement 10 runs of 15 individual measurements were done.

2.12. Mass spectrometry analysis

Gel band of 12 kD was digested with modified trypsin (Promega), injected one a Dionex RSLC nano LC system (Thermo Fisher Scientific), and analyzed on-line with a LTQ-Orbitrap mass spectrometer (Thermo Electron). A database search was performed with Xtandem cyclone (2011.12.01.1, http://www.thegpm.org/TANDEM/) using the X!Tandem Pipeline (3.2.0, http://pappso.inra.fr/bioinfo/xtandempipeline/). Histag–Shadoo protein sequence, the Uniprot KB database (514 212 entries, version 2010), and the contaminant database (trypsin, keratins, ...) were used for analysis.

3. Results

3.1. Sho aggregation is pH dependent

Sho produced in *E. coli* was purified as described under "Materials and Methods" and subjected to SDS–PAGE analysis. Coomassie Bleu staining revealed a band of about 12 kDa that corresponded to the theoretical molecular mass of Sho (Fig. 1A). Detected protein was further submitted to high resolution mass spectrometry analysis, which identified the band as mouse Sho of 12.2 kDa (22 unique peptides corresponding to a sequence coverage of 45%).

After purification, Sho was desalted against various buffers and its structure and aggregation state were assessed over a broad pH-range, from pH 3.35 to pH 8.0. DLS measurements of the Sho mean hydrodynamic diameters (R_H) showed that Sho was monomeric at acidic pH (Fig. 1B). The R_H was found to range from 1.5 to 5 nm at pH $\leqslant$ 6, as expected for a small protein of about 12 kDa. Upon prolonged incubation in acidic buffers (1–3 weeks), R_H of Sho did not change compared to those measured in freshly prepared solutions (data not shown), suggesting that Sho is monomeric and stable at acid pH. However, at pH $\geqslant$ 7, Sho aggregated to particles with diameters of a few microns and tended to precipitate (Fig. 1B).

The pH-dependence of the Sho secondary structure was analyzed by CD measurements carried out on protein incubated at pH ranging from 3.35 to 8.0. The far-UV spectrum of Sho exhibited shape characteristics of a random coil conformation in whole pH range. No evidence of stable secondary structure was found, but monomeric forms had a more pronounced minimum at 198 nm than that of the aggregated forms (Fig. 1C). This is probably due to the protein precipitation at basic pH. Each of these experiments was repeated with at least three independent protein preparations and always gave the same results.

A previous study of Sho structural assembles showed that Sho forms amyloid fibers upon two-week incubation at pH 7.4 without recourse to any chemical treatment [8]. Thus, using a ThT analysis, Sho amyloid fiber formation was checked after two-week incubation in whole pH range (pH 3.35–8.0). No ThT increase was detected in protein preparations at pH < 7. However, at pH $\geqslant$ 7, Sho appeared to spontaneously form amyloidal fibers since intensity of ThT fluorescence increased up to threefold times at pH 8, compared to controls (Fig. 1D).

Taken together, the results from Fig. 1 indicated that Sho was a stable, monomeric and unstructured protein in acidic solutions, but aggregated into large assembles at pH $\geqslant$ 7. To further investigate Sho in membrane-mimicking conditions measurements were done at pH 5.

3.2. Sho binds to negatively charged membranes

The interaction of Sho with artificial membranes was monitored by fluorescent spectroscopy of its tryptophan residues. Sho has 5 Trps within its sequence. The λ_{max} of emission of a Trp excited at 292 nm reflects the polarity of its environment. In hydrophilic solutions, the λ_{max} can reach 355 nm, while in hydrophobic environment, as happened when Trp is inserted into a lipidic bilayer,

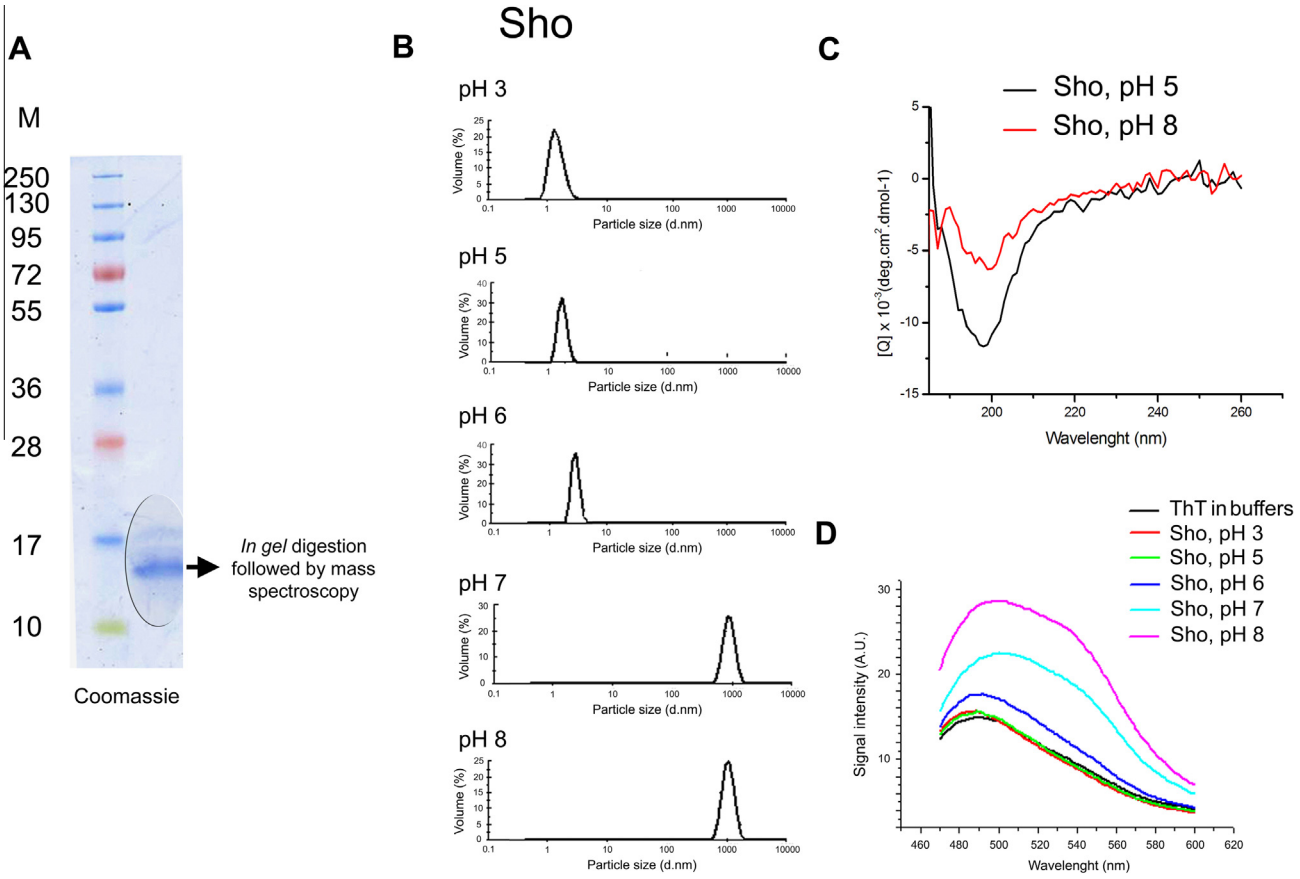

Fig. 1. Expression and purification of Sho and detection of Sho aggregates. (A) 3 μg of the purified protein was subjected to the SDS–PAGE electrophoresis and Coomassie bleu stained. The relative molecular weight (shown in kDa) was determined by reference to marker proteins. Allindicated bands of detected protein, at about 12 kDa, were cut from the gel and subjected to the high resolution mass spectroscopy analysis. (B) Dynamic Light Scattering (DLS) of purified Sho protein (2 μM) over a range of pH values from 3 to 8, recorded at 20 °C. (C). Circular Dichroism of Sho (20 μM) at pH 5 (black) and pH 8 (red). Spectra were recorded at 20 °C. (D). Measurements of the fluorescence intensities of ThT staining of amyloids formed by the Sho (2 μM) incubated for 2 weeks in different buffers with pH ranging from 3 to 8. No chemical treatment of the protein. AU, absorbance units. (For interpretation of the references to color in this figure legend, the reader is referred to the web version of this article.)

the λ_{max} shifts to 320 nm. Since Sho is an unstructured protein its Trps are expected to be flexible and exposed to the buffer solution. Indeed, in sodium acetate buffer, pH 5, Sho showed the λ_{max} of Trp emission at 353 nm (Fig. 2A, black line). Similarly, PrP and Nter-PrP showed a fluorescence maximum at 352 nm and 354 nm, respectively (Fig. 2A, black lines). The full length PrP contains seven Trp residues that are located within its N-terminal.

When Sho, PrP or Nter-PrP were incubated with membrane vesicles solely consisting of zwitterionic PC, no measurable λ_{max} shift was observed (Fig. 2A, red lines), suggesting the lack of protein-membrane interactions. However, fluorescence spectra markedly changed when proteins were incubated with negatively charged vesicles containing acidic PS. As shown in the Fig. 2A (red lines) the emission spectra of proteins are shifted to shorter wavelengths upon interaction with PS liposomes (from 353 to 338 nm; from 352 to 346 nm and from 354 to 348 nm for Sho, PrP and Nter-PrP, respectively). The fluorescent intensities of Sho and PrP decreased upon interactions with PS. Observed blue shifts reflect the increase of the hydrophobicity of the Trp environment and thus suggest the binding of Sho, PrP and Nter-PrP to the PS membranes.

To further verify the association of Sho with membranes, Sho was incubated either with PC or PS vesicles for 2 weeks at 4 °C and then ultracentrifuged to separate lipidic from soluble fraction. Separated fractions were probed for the presence of proteins. For comparison, PrP and Nter-PrP were also incubated with liposomes. Fig. 2B shows that Sho, as well as PrP, and Nter-PrP were detected in both aqueous and lipid fractions when incubated with PC vesicles. However, after incubation with negatively charged PS liposomes, all three proteins were detected only as lipid-bound.

3.3. Anionic liposomes induce Sho fibrilization

Using the ThT assay the presence of amyloid fibers were tested for Sho, PrP and Nter-PrP incubated with liposomes. When incubated with PC liposomes, proteins showed no increase in ThT fluorescence compared to liposomes alone (Fig. 3A). However, proteins incubated with PS liposomes gradually converted into fibrils as monitored by the increasing ThT signal. We observed that fluorescent intensity increased 8-fold for PrP, and 3.5-fold for both Sho and PrP-Nter after 2 weeks incubation with PS liposomes (Fig. 3A, green lines). To confirm the effect of acidic lipids on Sho polymerization, Sho was incubated with liposomes containing increasing content of PS. Fig. 3B shows that signal of ThT staining increased together with the PS/PC ratio in liposomes.

The secondary structure of Sho in those membrane-like environments was studied by CD spectroscopy. The CD spectrum of Sho incubated with liposomes exclusively made of neutral PC lipids overlaped the spectrum of Sho alone in the buffer solution, reflecting the absence of interaction (Fig. 3C). However, in the presence of acidic liposomes, there was a decrease in the magnitude of the negatively ellipticity above 195 nm and a small shift with a minimum towards wavelengths above 200 nm. The spectral changes were proportional to the increasing content of PS in mixed liposomes, strongly suggesting that negatively charged lipid environment produces some rearrangement in the Sho conformation.

Similarly, giant PS liposomes preincubated with Sho exhibited a fluorescent staining (Fig. 3D). This suggests the presence of amyloid structure associated with liposomes. In contrast no staining was observed with liposomes or proteins alone. The microscopic observation also showed that upon interaction with Sho, fewer PS liposomes were observed and exhibited smaller diameters than that in absence of Sho. This suggests the destabilization of PS giant liposomes upon binding Sho. In contrast, no change in morphology nor any ThT fluorescence was observed when Sho was added to PC liposomes (data not shown).

3.4. Liposome destabilizations and lipid–protein complex formation

To address variations in liposome sizes upon Sho binding, we generated small lipid vesicles and mixed them with Sho. Without proteins, both PS and PC extruded liposomes had R_H of about 100 nm (Fig. 4A, black lines). Interestingly, after incubation with Sho, the R_H of PS liposomes was slightly shifted to about 150 nm, while almost no changes in liposome sizes could be observed with PC vesicles (Fig. 4A green lines). This suggests that Sho partially aggregated PS but not PC liposomes. In comparison, PrP aggregated and fragmented PS liposomes giving one population of vesicles of about 700 nm diameters, and the second of about 90 nm (Fig. 4A), red lines). However, PrP did not destabilize PC liposomes (Fig. 4A, red lines). DLS measurements confirm that both Sho and PrP interacted with liposomes of negative net charge but not with zwitterionic.

To further gain insight into the mechanism of Sho interaction with PS liposomes, negatively stained lipid/protein preparations were observed under electron microscopy. Images in Fig. 4B show

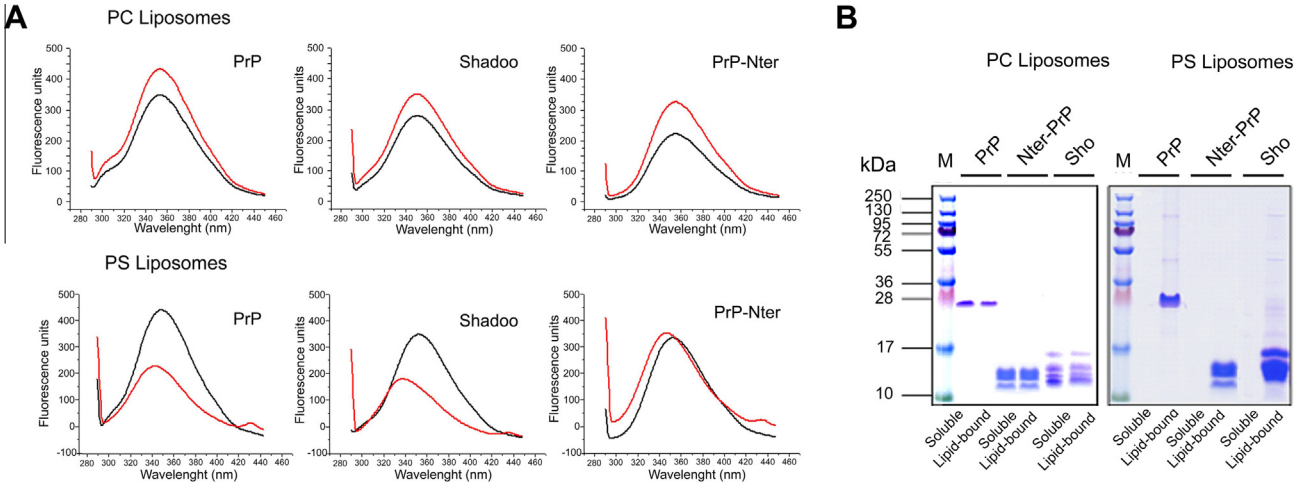

Fig. 2. Sho binds anionic but not neutral liposomes. (A) Liposomes (diameter, 100 nm) were incubated with proteins in 20 mM sodium-acetate buffer, pH 5, for 2 weeks at 4 °C. Protein Trp spectra were recorded before (black) and after incubation (red). Note that Trp fluorescence maximum shifted only when proteins were incubated with anionic PS liposomes. (B) Sho, PrP and Nter-PrP were incubated with PC or PS liposomes for 2 weeks at 4 °C. Membrane-associated (lipid-bound) proteins were separated from free proteins (soluble) by ultracentrifugation. Note that all three proteins preferentially bind to the phospholipid vesicles of negative net charge. (For interpretation of the references to color in this figure legend, the reader is referred to the web version of this article.)

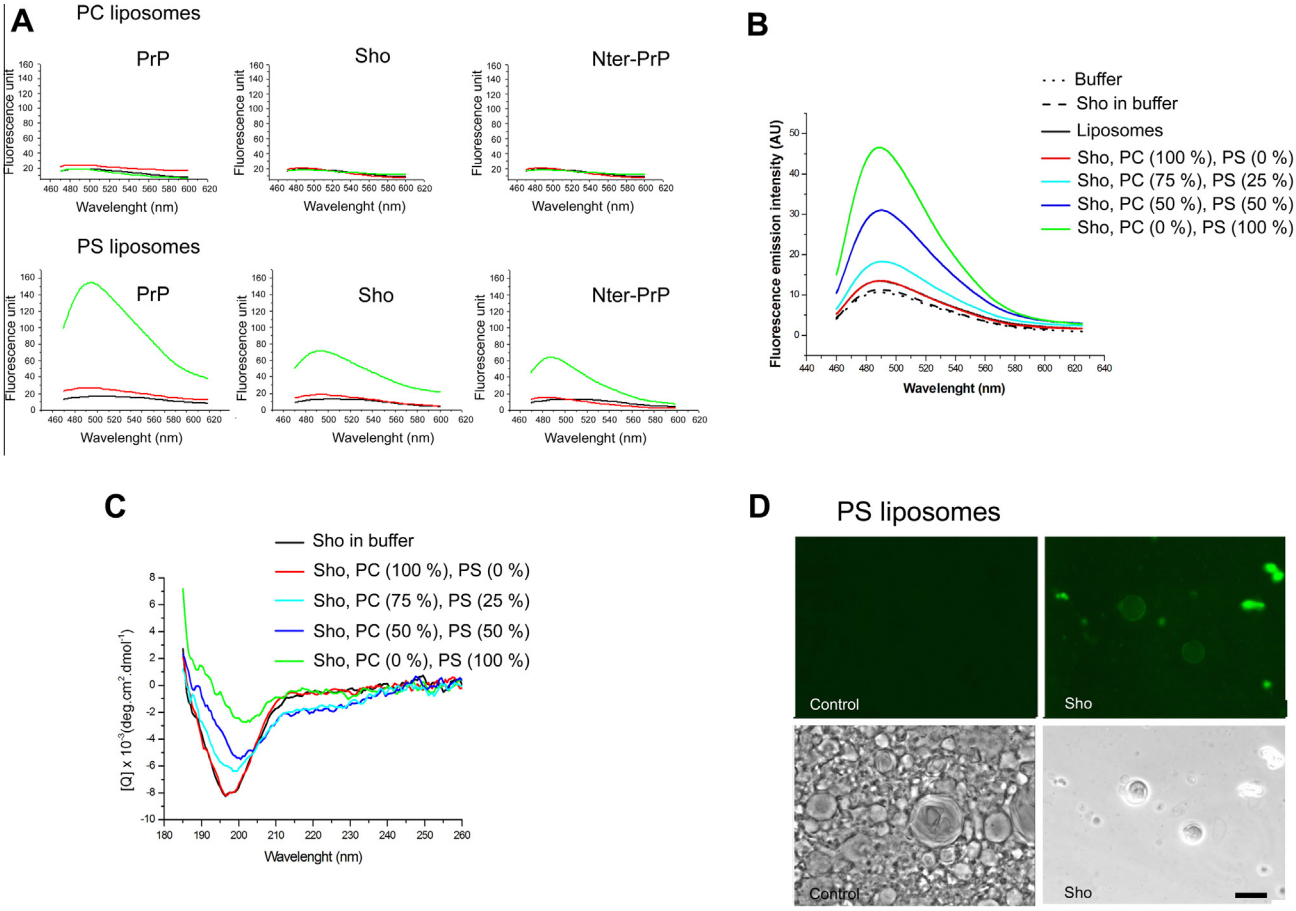

Fig. 3. Sho forms amyloid fibers upon binding anionic lipidic vesicles. (A) Emission fluorescent spectra of ThT (100 μM) of Sho, PrP and Nter-PrP (2 μM each) incubated with PC or PS liposomes (0.3 mg/ml each) in 20 mM sodium-acetate buffer, pH 5. Black: liposomes alone; Red: proteins immediately after mixing with liposomes; Green: proteins incubated for 2 weeks with liposomes. (B) ThT spectra of Sho (20 μM) incubated for 2 weeks with liposomes containing increasing amounts of PS (0–100%) at the expense of PC (100–0%). Total lipid concentration, 1 mg/ml. (C) Representative circular dichroism spectra of Sho (40 μM) incubated for 2 weeks with liposomes (1 mg/ml) containing increasing amounts of PS (0–100%) at the expense of PC (100–0%). (D) Fluorescent (top row panels) and optical (bottom row panels) visualizations of giant PS liposomes (0.5 mg/ml) stained with ThT (100 μM). Control preparation, liposomes alone. Sho preparation, liposomes incubated for 2 weeks with Sho (20 μM). Bar, 200 nm. (For interpretation of the references to color in this figure legend, the reader is referred to the web version of this article.)

fibrillar structures connected to vesicles. Indeed, each fiber was associated with one or few lipid vesicles. Fibers were often found growing on the surface of a single liposome or attached endwise with a vesicle. This suggests that nucleation of filaments takes place at the vesicles. PS liposome sizes were of about 150 nm, which is comparable to diameters determined by DLS (Fig. 4A). It was difficult to find intact spherical vesicle. Instead, vesicles of collapsed or distorted morphology were observed. The rough morphology of fibers from Fig. 4B suggests the transfers of lipids from vesicles to fibers, and the formation of supramolecular lipoprotein complexes. In contrast, PC liposomes failed to induce filament formation (data not shown).

4. Discussion

Lipid bilayers may act as an effective catalyst of protein fibrillogenesis [5,11–13]. Studies to date have reported the importance of the membrane lipid composition on providing a specific environment where proteins assemble into profibrillar and fibrillar structures [14]. Here, we first showed that Sho protein spontaneously undergoes aggregation and polymerization at physiological and basic pHs. At acidic pH, Sho is a stable, monomeric protein deprived of ordered secondary structure. We, further, showed that the mode and extend of Sho binding to membranes is determined by the bilayer net charge. Finally, we established that Sho bound to an anionic lipid surface can assembly into fibrillar structures and that this fibrillization is probably accompanied by the alternation in bilayer structure and the uptake of lipids by the forming fibers.

Similarly to PrP, Sho contains a conserved internal HD and a series of N-terminal tandem repeats rich in positively charged residues [7]. Regardless their structural similarities, Nter-PrP is soluble at physiological pH, while Sho tends to be aggregated and form insoluble amyloid-like fibers at pH $\geqslant$ 7. Sho is devoid of cysteine residues that can stabilize protein conformation by forming disulfide bridges and appears to be naturally flexible unstructured protein. In consequence, there was no need for chemical treatment of Sho to initiate its fibrillization, as was shown before [8].

At acidic pH, Sho forms amyloid-like fibers upon extended incubation with anionic membranes, as ascertains here by Trp fluorescent measurements, ultracentrifugation, ThT staining and electron microscopy. Sho binding to membranes is probably mediated by electrostatic interactions and involved Sho's basic repeat region interactions with the polar region of phospholipid head-groups. In contrast, no affinity of Sho to bind zwitterionic liposomes was observed. This lipid specificity was also observed for PrP and its N-terminal peptide, and for some other amyloid forming proteins

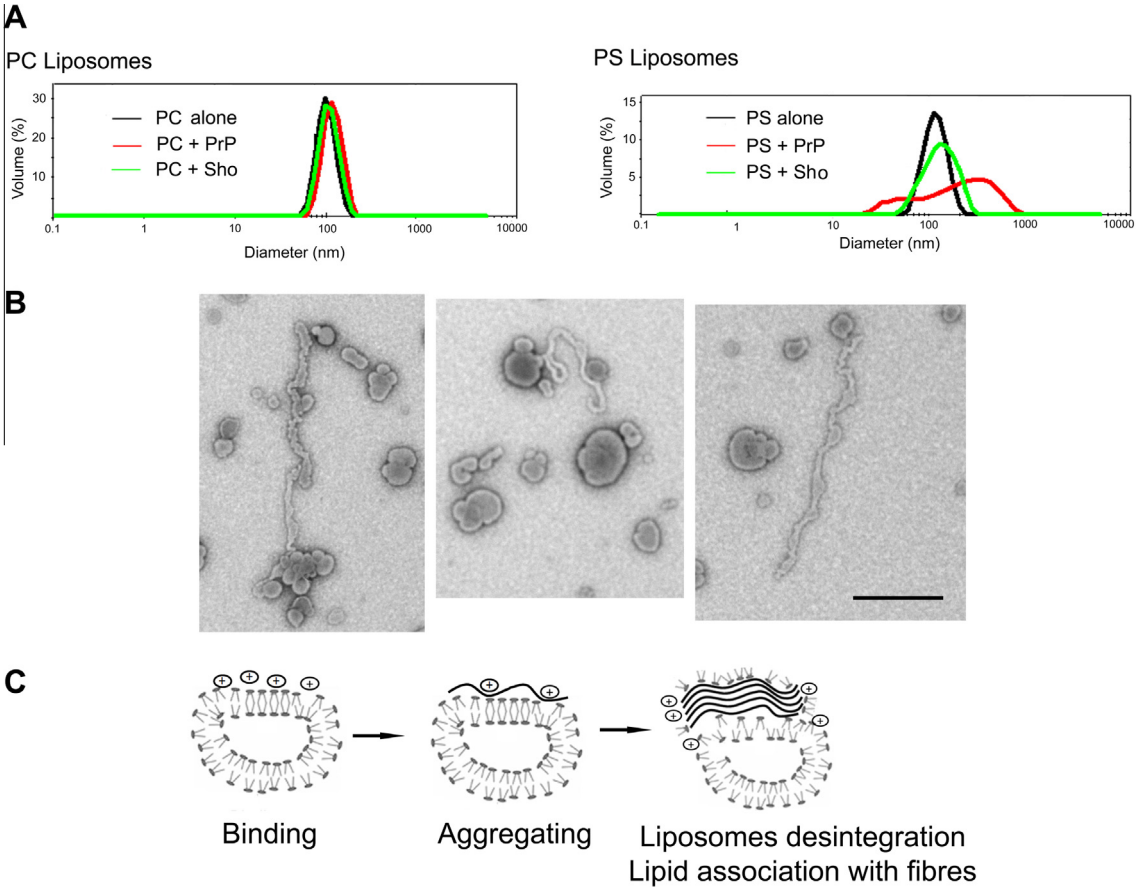

Fig. 4. Liposomes destabilization upon binding Sho and formation of lipoprotein complexes. (A) Size distribution of extruded liposomes (0.5 mg/ml) alone (black) and incubated for 2 weeks with 2 μM Sho (green), or 2 μM PrP (red) in 20 mM sodium-acetate buffer, pH 5 (protein/lipid ratio 1:50). (B) Electron microscopy of negatively stained extruded PS liposomes (0.7 mg/ml) incubated with 20 μM Sho for 2 weeks in 20 mM sodium-acetate buffer, pH 5. Bar, 500 nm. (C) Schematic model for Sho interaction with anionic membranes. Firstly, electrostatic adsorption gives binding of the positively charged Sho protein to the negatively charged membrane surface. Secondly, the electrostatic interactions increase significantly concentration of surface-associated Sho protein compared to bulk concentration, which allow a conversion of Sho monomers into amyloid-like fibers. Fibers destabilize liposome integrity yielding to the dissociation of lipids from the lipid bilayer. Finally, dissociated lipids are integrated into the Sho fibers. (For interpretation of the references to color in this figure legend, the reader is referred to the web version of this article.)

[5,14]. The charge of membranes plays an important role in protein–lipid interactions. For instance, negatively charged lipids such as PS, or sphingomyelin were shown to increase the content of β-sheets structure and facilitate protein aggregations; while some neutral lipids as PC or cholesterol may protect against conversion [5,15].

Previous studies revealed that amyloid fibers may incorporate lipids *in vitro* [12,16] and *ex vivo* [17]. Our fluorescent microscopy visualized by ThT and electron microscopy demonstrated that Sho fibers colocalized with lipids from disintegrated PS liposomes. We can hypothesize that the positively charged Sho molecules after binding on the surface of the negatively charged membrane could result in the wrapping of the Sho fibers by PS lipids (Fig. 4C). The tight packing in these lipoprotein assemblies would lower the overall free energy of the amyloid, and further increase amyloid stability.

Sho expression levels are decreased in prion diseases [10,18]. Sho ability to polymerize when bound to acidic membrane may be relevant for the early stages of the infection. Experiments aimed to check whether polymerized Sho and/or supramolecular lipo-Sho complexes may recruit PrP for polymerization or, in contrast, play a protecting role should be underway to find Sho biological relevance. Improving our understanding of these multimolecular interactions in prion diseases will provide new insights into amyloidosis pathogenesis.

Acknowledgments

We thank Natalie Doude and David Westerway (University of Alberta) and Michel Brémont (INRA) for providing us with Sho cDNA and BL21Sol, respectively; Christine Longin (INRA) for TEM assistance. Stephane Biacchesi (INRA) for OM assistance and critical reading of the manuscript; Rachel Young (Institut Gustave Roussy) for critical reading of the manuscript.

References

[1] S.B. Prusiner, Novel proteinaceous infectious particles cause scrapie, Science 216 (1982) 136–144.
[2] S.B. Prusiner, M.P. McKinley, K.A. Bowman, D.C. Bolton, P.E. Bendheim, D.F. Groth, G.G. Glenner, Scrapie prions aggregate to form amyloid-like birefringent rods, Cell 35 (1983) 349–358.
[3] A. Kraus, B.R. Groveman, B. Caughey, Prions and the potential transmissibility of protein misfolding diseases, Annu. Rev. Microbiol. 67 (2013) 543–564.
[4] A.R. Walmsley, F. Zeng, N.M. Hooper, The N-terminal region of the prion protein ectodomain contains a lipid raft targeting determinant, J. Biol. Chem. 278 (2003) 37241–37248.
[5] S. Steunou, J.F. Chich, H. Rezaei, J. Vidic, Biosensing of lipid–prion interactions: insights on charge effect, Cu(II)-ions binding and prion oligomerization, Biosens. Bioelectron. 26 (2010) 1399–1406.
[6] D.R. Borchelt, A. Taraboulos, S.B. Prusiner, Evidence for synthesis of scrapie prion proteins in the endocytic pathway, J. Biol. Chem. 267 (1992) 16188–16199.

[7] D. Westaway, N. Daude, S. Wohlgemuth, P. Harrison, The PrP-like proteins Shadoo and Doppel, Top Curr. Chem. 305 (2011) 225–256.
[8] N. Daude, V. Ng, J.C. Watts, S. Genovesi, J.P. Glaves, S. Wohlgemuth, G. Schmitt-Ulms, H. Young, J. McLaurin, P.E. Fraser, D. Westaway, Wild-type Shadoo proteins convert to amyloid-like forms under native conditions, J. Neurochem. 113 (2010) 92–104.
[9] J.C. Watts, B. Drisaldi, V. Ng, J. Yang, B. Strome, P. Horne, M.S. Sy, L. Yoong, R. Young, P. Mastrangelo, C. Bergeron, P.E. Fraser, G.A. Carlson, H.T. Mount, G. Schmitt-Ulms, D. Westaway, The CNS glycoprotein Shadoo has PrP(C)-like protective properties and displays reduced levels in prion infections, EMBO J. 26 (2007) 4038–4050.
[10] J.C. Watts, J. Stöhr, S. Bhardwaj, H. Wille, A. Oehler, S.J. Dearmond, K. Giles, S.B. Prusiner, Protease-resistant prions selectively decrease Shadoo protein, PLoS Pathog. 7 (2011) e1002382.
[11] M. Necula, C.N. Chirita, J. Kuret, Rapid anionic micelle-mediated alpha-synucleinfibrillization *in vitro*, J. Biol. Chem. 278 (2003) 46674–46680.
[12] Y.A. Domanov, P.K. Kinnunen, Islet amyloid polypeptide forms rigid lipid–protein amyloid fibrils on supported phospholipid bilayers, J. Mol. Biol. 376 (2008) 42–54.
[13] C.N. Chirita, M. Necula, J. Kure, Anionic micelles and vesicles induce tau fibrillization *in vitro*, J. Biol. Chem. 278 (2003) 25644–25650.
[14] M. Stefani, Biochemical and biophysical features of both oligomer/fibril and cell membrane in amyloid cytotoxicity, FEBS J. 277 (2010) 4602–4613.
[15] N. Sanghera, M.J. Swann, G. Ronan, T.J. Pinheiro, Insight into early events in the aggregation of the prion protein on lipid, membranes, Biochim. Biophys. Acta 1788 (2009) 2245–2251.
[16] H. Zhao, A. Jutila, T. Nurminen, S.A. Wickström, J. Keski-Oja, P.K. Kinnunen, Binding of endostatin to phosphatidylserine-containing membranes and formation of amyloid-like fibers, Biochemistry 44 (2005) 2857–2863.
[17] G.P. Gellermann, T.R. Appel, A. Tannert, A. Radestock, P. Hortschansky, V. Schroeckh, C. Leisner, T. Lütkepohl, S. Shtrasburg, C. Röcken, M. Pras, R.P. Linke, S. Diekmann, M. Fändrich, Raft lipids as common components of human extracellular amyloid fibrils, Proc. Natl. Acad. Sci. USA 102 (2005) 6297–6302.
[18] D. Westaway, S. Genovesi, N. Daude, R. Brown, A. Lau, I. Lee, C.E. Mays, J. Coomaraswamy, B. Canine, R. Pitstick, A. Herbst, J. Yang, K.W. Ko, G. Schmitt-Ulms, S.J. Dearmond, D. McKenzie, L. Hood, G.A. Carlson, Down-regulation of Shadoo in prion infections traces a pre-clinical event inversely related to PrP(Sc) accumulation, PLoS Pathog. 7 (2011) e1002391.